ISBN: 978-3-95450-216-5 doi:10.18429/JACoW-eeFACT2018-TUYAA01

HIGH CURRENTS EFFECTS IN DAΦNE

C. Milardi†, D. Alesini, S. Bini, A. Drago, A. Gallo, A. Ghigo,
S. Guiducci, M. Serio, A Stella, M. Zobov, LNF-INFN, Frascati, Italy
F. Marcellini, PSI, Villigen, Switzerland
P. Raimondi, ESRF, Grenoble, France

Abstract

DAΦNE, the Italian lepton collider, operates routinely with high intensity electron and positron colliding beams. The high current multi-bunch beams are stored in two independent rings, each of them 97 m long, and are distributed into 100÷110 contiguous buckets out of the 120 available, spaced by only 2.7 ns.

Since its construction, DAΦNE has been operated in different configurations which, overall, allowed to store currents up to 1.4 A and 2.45 A in the positron and in the electron beam respectively. To this day DAΦNE holds the record for the highest electron beam current ever stored in particle factories and modern synchrotron radiation sources.

The DAΦNE experience, in terms of beam dynamics optimization aimed at achieving the high intensity beams, is presented with special emphasis on the *e-cloud* related issues which represent the dominant effect limiting the positron beam current.

INTRODUCTION

DAΦNE [1, 2] is an accelerator complex consisting of a double ring lepton collider working at the energy of the Φ-resonance, (1.02 GeV) and an injection system. The collider includes two independent rings, each ~97 m long.

The two rings share an interaction region (IR), where the detector on duty is installed. A full energy injection system, including an S-band LINAC, 180 m long transfer lines, and an accumulator/damping ring provides fast and high efficiency electron–positron injection in topping-up mode.

Since its construction DAΦNE has been manly operated in two configurations, differing essentially for the approach to the beam-beam interaction. In fact, till 2006, the main rings shared two ≈10 m long interaction regions, although only one detector at a time was taking data. Due to the common beam pipe, the two beams collided with a rather small horizontal angle, of the order of 25 mrad, which was also compliant with the Piwinski criterion [3]. During this initial phase, the collider performances have been significantly improved by several progressive upgrades and a wide program of machine measurements and studies, aimed at pointing out the physics processes limiting the maximum achievable current and luminosity, has been undertaken. This activity largely contributed to define a proposal for an original collision scheme based on large Piwinski angle and *Crab-Waist* (*CW*) compensation of the beam-beam interaction [4, 5]. In 2006 the novel approach to collision has been implemented on DAΦNE during a six months shutdown planned to install a compact detector without longitudinal magnetic field, offering an optimal simplified environment to test the new configuration: the SIDDHARTA experiment.

The parameter of the DAΦNE collider in the nominal and in the *CW* configurations are reported in Table 1.

Table 1: DAΦNE Beam Parameters

	DAΦNE native (2000÷2006)	DAΦNE CW Since 2007
Energy (MeV)	510	
β^*_y (cm)	1.8	0.85
β^*_x (cm)	160	23
σ^*_x (μm)	760	250
σ^*_y (μm) low current	5.4	3.1
σ_z (cm)	2.5	1.5
Bunch spacing (ns)	2.7	
Damping times τ_E, τ_x (ms)	17.8/36.0	
Cros. Angle $\theta_{cross}/2$ (mrad)	12.5	25
Pwinski Angle ψ (mrad)	0.6	1.5
ε (mm mrad)	0.34	0.28
RF frequency [MHz]	368.26	368.667
Harmonic number	120	
L •10^{32} (cm^{-2} s^{-1})	1.5	4.36

HIGH CURRENT DESIGN STRATEGY

The efforts aimed at achieving high intensity beams and at optimizing beam quality have been comparable to the ones invested in the beam-beam interaction approach.

Since the design stage all the main ring vacuum components have been specified in order to store large total current in a large number of bunches, which required special emphasis on vacuum and collective effect related topics.

Each ring vacuum chamber [6] consists of 4 arcs and straight sections. The chamber of the arcs is made by a special Al-Mg alloy (Al 5083 H321), while the straight section ones use a slightly different composition Al-Si alloy (Al 6082 T6). The dipole and wiggler beam pipes in the arcs are all equipped with antechambers and synchrotron radiation absorbers in order to improve pumping efficiency.

It is well known that collective instabilities in accelerators mostly come from an intense particle beam electromagnetically interacting with its vacuum chamber environment. This interaction, which can easily drive the beam to instability, is described by the wakefield (time domain) and beam-coupling impedance (frequency domain) concepts. Hence the need for a detailed evaluation of the impedance impact on single and multibunch dynamics [7]. Since the

† catia.milardi@lnf.infn.it

ISBN: 978-3-95450-216-5 doi:10.18429/JACoW-eeFACT2018-TUYAA01

very beginnings the machine design approach aimed at reducing as much as possible the number of vacuum chamber elements trapping parasitic High Order Mode (HOM) able to drive multi-bunch instabilities, and at pointing out technical solutions suitable to damp HOMs and instabilities as well. This approach has been primarily pursued by properly designing the RF cavities [8]. They integrate a system of waveguides coupled to HOMs resonant fields that allow to absorb the power released by the beam into the trapped modes. The residual excitation of beam oscillation is damped by a bunch-by-bunch digital feedback system.

The most relevant resonating volumes and discontinuities such as bellows, pumping ports, spherical beam pipe at the interaction point etc. have been shielded with screens.

The resistive wall impedance and the contribution to the impedance of the main inductive elements have been carefully evaluated as well as their contribution to the power losses.

New designs and novel ideas were adopted for almost all principal vacuum chamber components: RF cavities [9, 10], shielded bellows [11], longitudinal feedback kickers [12], BPMs [13], DC current monitors [14], injection kickers [15], transverse feedback kickers and others [16]. For example, longitudinal feedback kickers similar to those developed for DAΦNE are routinely used in more than ten operating colliders and synchrotron radiation sources.

The transverse mode coupling instability threshold has been evaluated and, according to simulations, was an order of magnitude higher than the nominal bunch current.

HIGH CURRENT EXPERIENCE

Despite the careful design efforts beam measurements taken during commissioning outlined some relevant difference between e^- and e^+ beam dynamics.

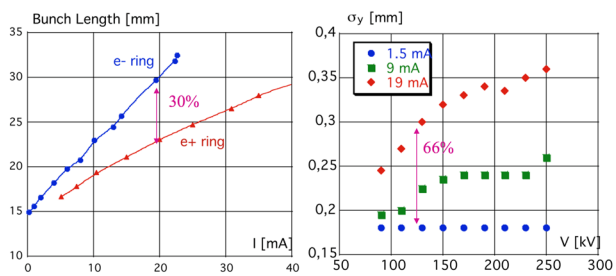

Figure 1: Comparison between e^- (blue dots) and e^+ (red dots) bunch length measurements as a function of the bunch current (left); measured vertical e^- beam size blow-up (right) as a function of the RF cavity voltage for different values of the bunch current.

First of all, at the nominal bunch current of 20 mA the e^- bunches were by about 30% longer than e^+ ones, as shown in Fig. 1. This had a direct impact in terms of geometric luminosity reduction due to the well-known hour-glass effect [17]. Moreover, for beams colliding with a horizontal crossing angle, as it is the DAΦNE case, synchro-betatron beam-beam resonances become stronger for longer bunches due to a larger Piwinski angle, thus limiting the maximum achievable beam-beam tune shift parameter.

The ring impedance has been estimated through bunch length measurements as a function of bunch current. Numerical fits based on a broadband model have shown that the beam coupling impedance of the two DAΦNE rings were different by approximately a factor of two. The measured impedance of the positron ring was $Z/n = 0.54\ \Omega$ to be compared with 1.1 Ω of the electron one. This difference produced several harmful consequences affecting the collider performances.

During ordinary operations also a transverse beam size blow-up, mainly in the vertical plane, was observed beyond the microwave instability threshold, see Fig. 2. This effect, which also exhibited a heavy dependence on the RF cavity voltage, as shown in Fig. 1, was clearly correlated with the longitudinal microwave instability, since it had the same threshold, the threshold was higher for larger values of the α_c parameter, see Fig. 2, and it was more harmful for the e^- ring which had a higher coupling impedance.

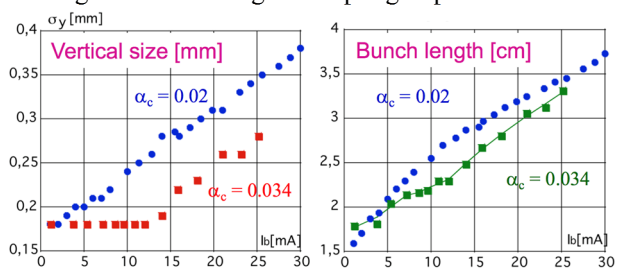

Figure 2: Measured vertical e^- beam size blow-up (left) and bunch length (right) as a function of bunch current for different momentum compaction (α_c) values.

Furthermore there was evidence of single bunch instability, mainly a longitudinal quadrupole oscillation, appearing at lower bunch current in the e^- ring. The quadrupole longitudinal instability has been controlled by a special technique implemented at DAΦNE [18] in the synchrotron (dipole) feedback system. The new technique consisted in shifting the Quadrature Phase Shift Keying (QPSK) modulated signal driving the feedback back end in order to damp both dipole and quadrupole beam motions.

NEGATIVE MOMENTUM COMPACTION

As far as high current issues are concerned, it is worth recalling the experimental test done at DAΦNE implementing a lattice with negative momentum compaction (α_c) in both rings [19].

In such configuration a considerable bunch shortening has been measured as predicted by numerical simulations. High single bunch currents have been stored in both beams, notably in the e^+ ring current up to 40 mA has been measured with large negative chromaticities, without any evidence of head-tail instability.

Concerning multi bunch dynamics, stable currents of the order of 1 A have been stored in both rings without any problem for RF cavities and feedback systems operation. Remarkably feedbacks were not necessary to store currents

ISBN: 978-3-95450-216-5 doi:10.18429/JACoW-eeFACT2018-TUYAA01

up to 400 mA in the e^- ring. The 1 A current limit was essentially due to saturation in the injection process that, due to the major lattice modifications, required careful optimization.

The encouraging results led to test collisions with the negative α_c lattice configuration. At first a comprehensive collision tuning allowed to reproduce the same values in terms of convoluted dimension of the interacting bunches at the IP, as for the positive α_c optics ($\Sigma_y \sim 8.2$ μm and $\Sigma_x \sim 1$ mm). Then currents have been progressively increased looking at the beam-beam phenomenology. The best luminosity results have been obtained with currents of the order of 300 mA in both beams, which gave a luminosity $L = 2.5 \times 10^{31}$ cm^{-2} s^{-1} corresponding to a specific luminosity of the order of $2.5 \cdot 10^{28}$ cm^{-2} s^{-1} mA^{-2}, a rather higher value if compared with the one ordinary measured with positive α_c optics; unfortunately the promising results were not confirmed at high currents. To our knowledge DAΦNE is the only collider to have implemented and studied collision with negative α_c.

BEAM DYNAMICS OPTIMIZATION

Years 2001÷2006

In order to cancel out the differences between e^- and e^+ rings the electrodes (ICEs) originally installed in the wiggler beam pipes of the e^- ring with the aim of neutralizing the ions of the residual vacuum, were removed. The activity was carried on during the shutdown propaedeutical to the installation of the FINUDA detector in 2006.

Beam measurements, after ICEs removal, confirmed that the e^- beam dynamics was almost comparable to that of the e^+ beam [20]. The e^- bunch length was 25÷30 % shorter, see Fig. 3, and there was no evidence of either quadrupole instability threshold or vertical beam blow-up at the operating bunch current (~ 15 mA).

This resulted in about 50% specific luminosity increase during the run for the FINUDA experiments [21].

Concerning multibunch operations, since 2002 it became possible to store current in 100 consecutive bunches after reducing the impact of parasitic crossing in the IR1 by: moderately reducing β^*_x and beam emittance, slightly increasing the crossing angle, varying $\theta_x/2$ from 12.5 to 14.5 mrad, and optimizing transverse and longitudinal feedback systems [22].

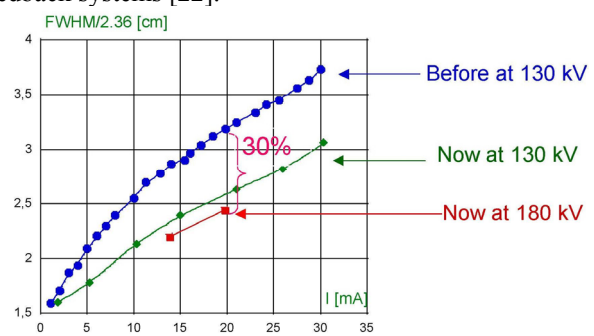

Figure 3: Bunch lengthening before (blue dots) and after (green and red dots) ICEs removal.

By the end of 2006, after the FINUDA run, also thanks to significant improvements to the non-linear optics [23, 24], the maximum stored currents were $I^- = 2.4$ A and $I^+ = 1.4$ A; while the maximum luminosity was achieved at current of the order of 1.5 A and 1.1 A for the e^- and the e^+ beam respectively, (see Table 2).

Crab-Waist Upgrade

By the end of 2006, in the framework of upgrades aimed at implementing the innovative *Crab-Waist* Collision Scheme [25] several vacuum elements were modified once again.

A new crossing section providing complete separation between the two beams replaced the second IR.

A new IR was designed [26] in order to implement a full separation between the two ring beam pipes just after the first defocusing quadrupole of the low-β, paying great attention to avoid all the possible discontinuities so as to keep the ring coupling impedance low. The number of bellows was also limited to the minimum necessary to compensate thermal strain and mechanical misalignments. There were four bellows per ring both in IR and in the crossing region. The vacuum chamber of the IR consisted of straight pipes merging in a *Y* shaped section. Special attention has been paid to the *Y-section* design since beam induced electromagnetic fields can generate trapped high order modes (HOM). Simulations have pointed out four possible HOMs, among them only the first was trapped and, even in the worst case, assuming the beam spectrum in full coupling with the trapped mode, the estimated released power was less than 200 W. Nevertheless, the *Y-section* was equipped with a cooling system to remove the heating due to the HOM [27].

Newly designed bellows were installed in the new IR and in the ring crossing section. The inner radius of bellows convolutions was ≈ 65 mm, the outer one 80 mm and the length ≈50 mm, see Fig. 4. They exploited innovative RF shield [28], necessary to prevent the discontinuity from acting as a cavity for the beam. The new RF shield was implemented by means of Ω shaped Be-Cu strips, installed all around two cylindrical aluminium shells fixed at the bellows ends.

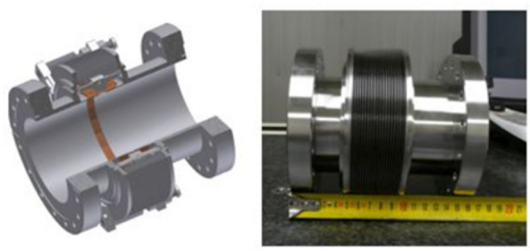

Figure 4: Copper-Beryllium strip shielded bellows, mechanical design (left) and real device (right).

These shields replaced the old ones realized by using contiguous mini bellows. Electromagnetic simulations performed with the HFSS code in the frequency range from DC to 5 GHz showed that the new design reduced bellows contribution to the ring coupling impedance.

ISBN: 978-3-95450-216-5 doi:10.18429/JACoW-eeFACT2018-TUYAA01

The injection kickers, two in each ring, were replaced with new devices [29] based on tapered strips embedded in a rectangular cross section vacuum chamber allowing injection rate, in principle, up to 50 Hz, see Fig. 5.

Figure 5: The new injection kicker under test (left) and installed on the electron ring (right).

Moreover, a smooth beam pipe and tapered transitions reduced the kickers contribution to the total ring coupling impedance. All these features were intended to improve the maximum storable currents, colliding beams stability and background on the experimental detector during injection.

The vacuum chamber components modifications for the CW experiment brought another relevant factor in the coupling impedance reduction.

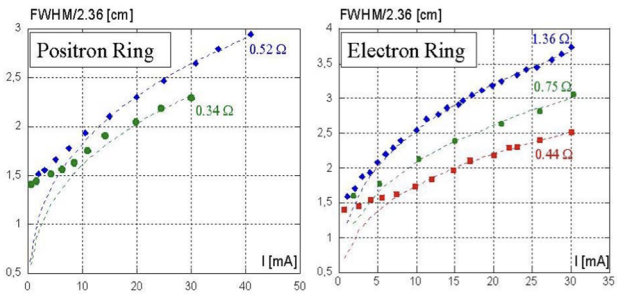

Figure 6: Bunch lengthening for the e^+ beam (left) before (blue) and after (green) the *CW* upgrade; bunch lengthening for the e^- beam (right) for the native ring setup (blue), after ICEs removal (green) and after *CW* upgrade (red).

As one can see in Fig. 6 by comparing the green and red curves, bunches in the electron ring were by about 20% shorter with respect to the previous FINUDA run.

During the test run for the CW configuration with the SIDDHARTA experiment the maximum currents that have been stored were $I^- = 2.2$ A and $I^+ = 1.2$ A; while the peak luminosity, which was three times larger than in the past [30, 31], was achieved at current of the order of 1.47 A and 1.0 A for the e^- and the e^+ beam respectively, (see Table 2).

Crab-Waist for the Large KLOE-2 Detector

The remarkable improvements in terms of instantaneous and integrated luminosity achieved during the CW test opened new perspectives for physics research at DAΦNE, and a new run was planned for the upgraded KLOE-2 detector.

Several activities were undertaken [32] in view of the KLOE-2 preliminary run in 2010.

A new IR was designed [33] to cope with the requirements of the KLOE detector, which included a high intensity longitudinal field strongly perturbing beam dynamics and coupling the transverse betatron oscillations of the stored beams.

The leftover old-style bellows were replaced with new ones having lower impedance and providing long lasting shield contour uniformity when compressed.

Few ion clearing electrodes, still present in the electron ring and no longer used, were removed.

New electrodes (ECE) have been installed in the e^+ ring to mitigate the *e-cloud* induced effects.

The Collimator rectangular vacuum chambers, (20 mm high and 90 mm wide), were replaced by square ones (55 mm) to optimize their contribution to the ring impedance. Moreover, the new design allowed to move the blades closer to the beam, improving their effectiveness in intercepting the background otherwise hitting the experimental detector.

The new kicker developed for the transverse horizontal positron feedback was also used as a beam dumper. It was installed in the opposite section with respect to the IR and was intended to dump the beam in a controlled way reducing the radiation level in the area and avoiding dangerous detector trips.

Also in this case the ring impedance was estimated relying on bunch length measurements as a function of bunch current. Results have shown a bunch lengthening reduction of the order of 10% at a current of 20 mA with respect to the values attained during the test run with the CW scheme.

Bunch length is neither affected by the insertion of the beam collimators nor, on the positron ring, by the presence of the new electrodes for electron clearing, see Fig. 7. ECEs contribution to the inductive component of the ring impedance is negligible, as emphasised by bunch lengthening with current that, in the e^+ ring, was even lower than in the e^- one.

The RF cavity hardware was also reviewed developing a direct RF feedback system in the low-level RF. This allowed to reduce the cavity detuning angle, increasing the overall efficiency and limiting the reduction of the coherent '0-mode' synchrotron frequency with beam current. The power of the ring RF station was limited to ≃60 KW, with respect to the 180 kW nominal value, by decreasing the klystron HV in order to reduce the power consumption. The reduced RF power was nevertheless sufficient to sustain the stored current.

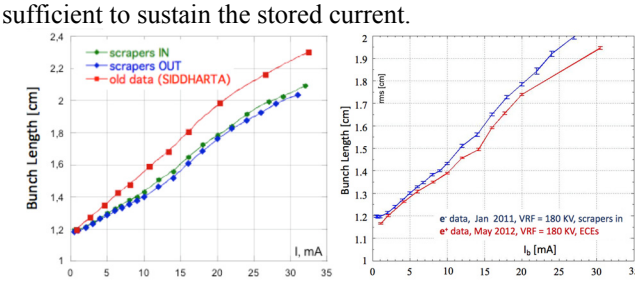

Figure 7: e^- beam bunch lengthening as a function of the bunch current for different e^- ring configurations (left); comparison between e^- and e^+ bunch lengthening after the *CW* upgrade for the KLOE-2 run (right).

ISBN: 978-3-95450-216-5 doi:10.18429/JACoW-eeFACT2018-TUYAA01

The four wigglers installed in each ring have been modified [34] to reduce the higher order multipoles of the magnetic field, and by removing a purpose built sextupole component, which had been efficiently used to implement a smooth and distributed chromaticity control.

Unfortunately, the preliminary run outlined a major fault in some bellows in the IR, which had lost electrical continuity causing anomalous beam induced heating of one of the two defocusing quadrupoles, ultimately resulting in a harmful random vertical tune-shift. For this reason, during the shutdown of 2013, intended to upgrade the detector, the vacuum chamber around the interaction point was replaced [35]. The new one had tapered transition between the thin ALBEMET sphere and the Al beam pipes, and included reshaped bellows with new designed RF contacts. Two cooling coils were added on the tapers and new
semi-cylindrical thin (35 mm) beryllium shields were placed inside the sphere.

Thereafter during collider operations, the e^- beam was still exhibiting the effects due to a microwave instability threshold appearing above a current of the order of ~10 mA per bunch, resulting in a widening of the transverse beam sizes. Such effect was quite moderate in single beam operation and became sometimes more harmful in collision due to the beam-beam interaction [36]. There was a plan to cure this effect by using an optics with higher momentum compaction α_c, but there was no time to implement it.

Furthermore, the quality of the e^- beam depended heavily on the mitigation of the effect induced by the ions of the residual vacuum, such effect is counteracted by leaving a suitable empty gap in the batch. The width of such gap is a compromise between opposite requirements posed by e^- beam dynamics and high luminosity. It depends greatly on the vacuum condition which improves with the stored beam dose. In fact, the best results in terms of luminosity have been achieved, by the second half of the run, through collisions of 106 consecutive bunches.

In general beam dynamics was affected by all the modifications implemented in the two rings.

Beam currents, especially the e^- one, were affected by longitudinal quadrupole oscillations. This instability was successfully kept under control by the QPSK based techniques as in the past. The environmental RF and DC noise coming from pickups, and leading to undesirable vertical beam size growth, was minimized by installing a low noise front end, designed in collaboration with SuperKEK feedback team, on the vertical feedback.

E-cloud Related Issues

Since the beginning of high current operations, the e^+ beam dynamics has been shown to be dominated by the *e-cloud* induced instabilities. The e^+ current was limited by several factors all related to the *e-cloud* phenomenology, such as: fast horizontal instability at high current, increase in the vertical beam size, tune-spread along the batch, and anomalous vacuum pressure rise with current in the arcs. Measurements and simulations showed how horizontal instability was triggered by the *e-cloud* formation in the dipoles and in the wigglers vacuum chambers [37].

The DAΦNE collider has been designed much before than the accelerator scientific community recognized the impact of the *e-cloud* on beam dynamics, for this reason some project options were not properly optimized as, for instance, the choice of Al for the vacuum chamber. In fact, Al has very high Secondary Electron Yield (SEY). Nevertheless, some other features played a positive role to contain the *e-cloud* formation. It is the case of the antechamber and the synchrotron radiation absorbers integrated in the dipole and wiggler vacuum chamber nominal design. It must also be considered that DAΦNE operates at rather low energy with high intensity multi-bunch beams, and very low bunch spacing, of the order of ~ 2.7 nsec. The energy emitted by synchrotron radiation each turn is of the order of 9.7 KeV which, due to the short ring circumference, corresponds to a quite high energy density.

Beside design concepts several countermeasures were adopted while operating DAΦNE, tuning rings and beam parameters, installing new devices, potentiating bunch-by-bunch transverse feedback systems, and last but not least securing optimal dynamic vacuum conditions, for instance, sublimating frequently the ring vacuum chambers.

A positive result was obtained lengthening the bunch by reducing the voltage of the RF cavity of the e^+ ring. Fig. 8 presents the behaviour of the pressure rise with the stored current, measured by two vacuum gauges installed on different arcs, as a function of the RF cavity voltage. Positive effects were obtained also moving ring chromaticity toward high positive values, and tuning the octupole magnets.

As far as devices are concerned, solenoidal coils were winded all around straight sections. The transverse horizontal feedback power was doubled (500 W now) providing ~40% increase in the kick strength. The horizontal feedback kicker was replaced with a device having double stripline length and reduced plate separation, providing larger shunt impedance at the low frequencies typical of the unstable modes.

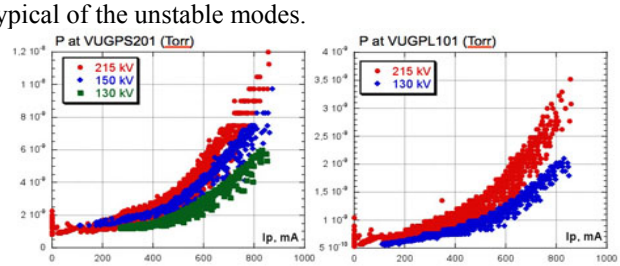

Figure 8: Pressure rise versus stored e^+ current in 2 different arcs as a function of the RF cavity voltage.

Moreover, the kicker was moved in a lattice position having a higher β_x value. On purpose designed electrodes [38] were installed inside dipole and wiggler vacuum chambers. The electrodes were checked in 2012, during the KLOE preliminary run. Several measurements and tests demonstrated their effectiveness in thwarting the *e-cloud* effects [39, 40]. Moreover, ECEs made possible a number

ISBN: 978-3-95450-216-5 doi:10.18429/JACoW-eeFACT2018-TUYAA01

of unprecedented measurements (*e-cloud* instabilities growth rate, transverse beam size variation, tune shifts along the bunch train) where the *e-cloud* contribution was clearly evidenced by turning ECEs on and off. Tests with ECEs also provided a useful framework to benchmark simulation codes.

The vertical beam size enlargement has been measured at the synchrotron light monitor by gradually turning off all the electrodes as shown in Fig. 9. The vertical size increased from about 110 μm with electrodes on to more than 145 μm with the electrodes off. This trend clearly indicated that the single bunch *e-cloud* instability was responsible for the vertical beam size growth.

The tune modulation along the batch induced by the *e-cloud* density variation [41] is reported in Fig. 10.

The fractional tunes progressively increase and reaches a steady state regime after ~20 bunches. In the horizontal plane the head-tail tune spread is about 0.006–0.008.

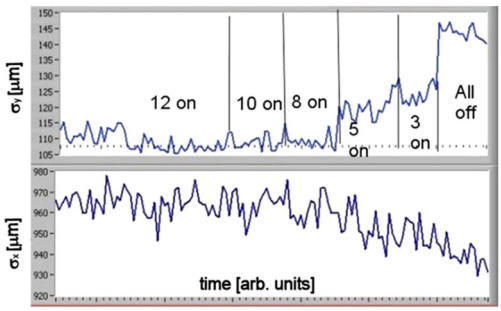

Figure 9: Beam dimension at the SLM turning progressively off all ECEs (I^+ = 500÷600 mA, 100 bunches).

Relying on simulations, this tune shift should correspond to an *e-cloud* density, in the wiggler sections, of the order of 10^{14} m^{-3}, a value significantly different than the one predicted by simulation. However, such discrepancy is consistent with a local *e-cloud* density in the vacuum chamber centre, close to the beam trajectory, higher by an order of magnitude with respect to the average density foreseen by the theoretical model.

When the ECEs are switched on the tune shift reduces by a factor of 2–3, but they do not cancel completely the tune spread. This can be explained reminding that the electrodes in the wigglers cover only 67% of their total length. In turn, as it is seen in Fig. 10(b), the vertical tune spread is notably smaller than the horizontal one and the ECEs almost completely cancel it. Still some vertical tune variation is observed while turning on and off the ECEs. This behaviour can be explained with the residual orbit variation observed during the measurements. In fact, the presence of high strength CW sextupoles leads mainly to the vertical tune shift of all bunches in the batch.

These first studies were all done by polarizing the stripline with a positive voltage in the range 0÷250 V. However, simulations indicated that a factor two higher voltage was required to completely neutralize the *e-cloud* density due to a e^+ current of the order of 1 A. For this reason, during the 2013 shutdown the electrode power supplies were replaced with devices providing a maximum negative voltage of 500 V. The change of polarity was intended to limit the current delivered by the power supplies.

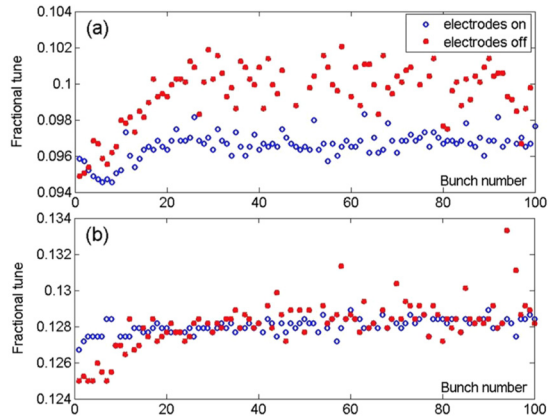

Figure 10: Measurements of horizontal (a) and vertical (b) fractional tunes along the batch at I^+~500 mA.

The new setup has been tested storing a ~ 700 mA current in 90 bunches spaced by 2.7 ns, and measuring the horizontal and vertical tune spread along the batch with the electrodes on and off. Results show a clear reduction of the tune spread in both planes, but especially in the horizontal one. Electrodes have been essential when the vacuum level in the e^+ ring was not optimal yet. At that stage, a careful tuning of each stripline polarization voltage was done in order to avoid sudden variation in the e^+ beam orbit. Then, progressively during the data taking, it was necessary to switched off several ECE due to their faulty behaviour. The KLOE-2 run finished with only 2 ECE fully operative, but, at that point, the benefits coming from the scrubbing process helped in keeping the *e-cloud* instabilities under control. A conclusive explanation of the process leading the ECEs to exhibit a faulty behaviour, after having worked for some time, is under way.

During the whole KLOE-2 run the maximum current stored in the e^+ beam has been of the order of I^+ ~ 1.2 A, although, at regime in collision, a current $I^+ > 0.95$ has been rarely injected; a value considerably lower than the one achieved during the previous DAΦNE's run periods.

Table 2: Beam Current Figures

	DAΦNE native (2001-2006)	**DAΦNE CW** SIDDHARTA (2007-2009)	**DAΦNE CW** KLOE-2 (2010-2018)
L_{peak}• 10^{32} ($cm^{-2}s^{-1}$)	1.5	4.4	2.38
I^- at L_{peak} (A)	1.5	1.47	1.18
I^+ at L_{peak} (A)	1.2	1.0	0.87
I^-_{MAX} (A)	**2.4**	2.2	1.7
I^+_{MAX} (A)	1.4	1.2	1.1
$N_{bunches}$	111	105	106

CONCLUSION

During the whole period of operations DAΦNE succeeded in providing and maintaining high intensity stable beams, thanks to the relevant design effort and to the

ISBN: 978-3-95450-216-5 doi:10.18429/JACoW-eeFACT2018-TUYAA01

constant improvement in terms of ring components, beam parameters and feedback systems.

Nevertheless, the e^- beam dynamics was clearly affected by a microwave instability threshold, whose implications had different impact for different collider configurations. It was more harmful during the last run for the KLOE-2 due to the many modifications implemented on the rings. Moreover, the quality of the e^- beam depended significantly on the mitigation of the effect induced by the ions of the residual vacuum. Despite it all, DAΦNE still holds the record for the highest electron beam current ever stored in particle factories and modern synchrotron radiation sources.

Concerning the e^+ current, it was strongly dominated by the *e-cloud* effects, which was mitigated by using solenoidal winding around the beam pipe, ECEs, and feedback systems. DAΦNE is the first collider to operate with and thanks to the ECEs. There is a clear evidence of a progressive reduction in the e^+ current which is evidently correlated to the Al beam pipe contamination consequent to the opening of the vacuum chambers for ring upgrade. We are convinced that ECEs and feedbacks systems upgrade have been fundamental in moderating the detrimental impact such effect.

AKCNOWELEDGMENT

Special thanks to the DAΦNE Technical Staff, they gave many relevant contributions to the work presented suggesting and implementing several technical solutions.

A special acknowledgment is due to Theo Demma for his valuable work about *e-cloud* effect.

REFERENCES

[1] G. Vignola *et al*., "Status report on DAΦNE", *Frascati Phys. Ser.*, Vol. 4, pp. 19-30, 1996.

[2] G.Vignola *et al.,* "DAΦNE, the first Φ-factory", in *Proc. 5th European Particle Accelerator Conference (EPAC96)*, pp. 22-26, 1996.

[3] A. Piwinski, "Storage Ring Luminosity as a Function of Beam-to-Beam Space and Crossing Angle", SLAC-TRANS-0067, DESY 67-7.

[4] P. Raimondi, D. Shatilov and M. Zobov, "Beam-beam issues for colliding schemes with large Piwinski angle and crabbed waist", e-*Print*: physics/0702033, LNF-07-003-IR, 2007.

[5] P. Raimondi, D. Shatilov and M. Zobov, "Suppression of beam-beam resonances in crab waist collisions", in *Proc. 11th European Particle Accelerator Conference (EPAC 2008)*, pp. 2620-2622, 2008.

[6] V. Chimenti *et al*, "The DAΦNE Main Ring Vacuum System", PAC93, pp. 3906-3908, 1993.

[7] M. Zobov *et al.,* "Collective Effects and Impedance Study for the DAΦNE F-Factory", LNF-95/041, July 1995.

[8] R. Boni *et al.,* "Stuy of the Parasitic Mode Adsorbers for the Frascati Φ-Factory RF Cavities", LNF-93/014 (P), April 1993.

[9] S. Bartalucci *et al*, "Analysis of Methods for Controlling Multibunch Instabilities in DAΦNE", Part. Accel. 48: 213-237, 1995.

[10] D. Alesini, *et al*, "Third Harmonic Cavity and RF Measure- ments for the Frascati DAΦNE Collider", Phys. Rev. ST Ac- cel. Beams **7**: 092001, 2004.

[11] G. O. Delle Monache, *et al*, "DAΦNE Shielded Bellows", Nucl. Instrum. Meth. A403: 185-194, 1998.

[12] A. Gallo, *et al*, "A Waveguide Overloaded Cavity as Longi- tudinal Kicker for the DAΦNE Bunch-by-Bunch Feedback System", Part. Accel. 52: 95-113, 1996.

[13] F. Marcellini, *et al*, "DAΦNE Broad-Band Button Electrodes", Nucl. Instrum. Meth. A402: 27-35, 1998.

[14] M. Zobov, *et al*, "Measures to Reduce the Impedance of Parasitic Resonant Modes in the DAΦNE Vacuum Chamber", Frascati Phys. Ser. **10**: 371-378, 1998.

[15] A. Ghigo, *et al*, "HOM Damping in the DAΦNE Injection Kicker", in Proceedings of 7th European Particle Accelera- tor Conference (EPAC2000), pp. 1145-1147.

[16] M. Zobov, *et al*, "Collective Effects and Impedance Study for the DAΦNE Φ-Factory", in KEK Proceedings 96-6, Au- gust 1996 (A), pp. 110-155.

[17] G. E. Fischer, SLAC report SPEAR-154, 1972.

[18] A. Drago *et al*., "Longitudinal quadrupole instability and control in the Frascati DAΦNE electron ring", *Phys. Rev. ST Accel. Beams*, Vol. 6, p. 052801, 2003.

[19] M. Zobov *et al*., "DAΦNE experience with negative momentum compaction",*EPAC06*, pp. 989-991.

[20] M. Zobov *et al.*, "Impact of Ion Clearing Electrodes on beam dynamics in DAΦNE", *JINST*, Volume 08, Issue 08, pp. 08002 (2007).

[21] C.Milardi *et al., PAC07*, pp.1457-1459, 2007.

[22] A. Drago *et al*., "100 Bunch DAΦNE Operation", Conf.Proc. C030512 (2003), pp. 366.

[23] C. Milardi *et al*., "Effects of nonlinear terms in the Wiggler magnets at DAΦNE", Conf.Proc. C0106181, pp. 1720-1722, 2001.

[24] C. Milardi *et al*., "Developments in linear and nonlinear DAΦNE lattice", Conf.Proc. C030512 (2003), pp. 2945-2947.

[25] F. Marcellini *et al*., "Coupling Impedance of DAΦNE Upgraded Vacuum Chamber", PAC08, p. 1661.

[26] C. Milardi *et al*., "DAΦNE Interaction Regions Upgrade", published in "Frascati 2007, Interaction regions for the LHC upgrade, DAΦNE and SuperB", 1-5, arXiv:0803.1450 [physics.acc-ph].

[27] F. Marcellini, "Design And Electromagnetic Analysis of the New DAΦNE Interaction Region", PAC07, p. 3988.

[28] S. Tomassini *et al*., "A New Rf Shielded Bellows For DAΦNE Upgrade", EPAC08, pp. 1706-1708, 2008.

[29] D. Alesini *et al*, D. Alesini, "Design, test, and operation of new tapered stripline injection kickers for the e^+e^- collider DAΦNE", Phys. Rev. ST Accel. Beams 13, 111002, doi: 10.1103/PhysRevSTAB.13.111002, 2010.

[30] C. Milardi *et al*., "Present status of the DAΦNE upgrade and perspectives", *Int. J. Mod. Phys*., Vol. A24, pp. 360-368, 2009;

[31] M. Zobov *et al*., "Test of crab-waist collisions at DAΦNE Φ–factory", *Phys. Rev. Lett*., Vol. 104, p. 174801, 2010.

[32] C. Milardi *et al*., "DAΦNE Developments For The Kloe-2 Experimental Run", IPAC10, pp. 1527-1529, 2010.

[33] C. Milardi *et al*., "High luminosity interaction region design for collisions inside high field detector solenoid", *JINST,* Vol. 7, p.T03002, 2012.

[34] S. Bettoni *et al.,* "Multipoles Minimization in the DAFNE Wigglers", in *Proc. 1st Int. Particle Accelerator Conf. (IPAC'10),* pp. 4665-4667.

[35] C. Milardi *et al*., "DAΦNE general consolidation and upgrade", IPAC14, pp. 3760-3762, 2014.

ISBN: 978-3-95450-216-5 doi:10.18429/JACoW-eeFACT2018-TUYAA01

[36] C. Milardi *et al*., "DAFNE tune-up for the KLOE-2 experiment", IPAC11, pp. 3687-3689, 2011.

[37] T.Demma *et al*., "A Simulation Study of the Electron Cloud Instability at DAΦNE", PAC09, pp. 4695-4697.

[38] D. Alesini *et al.,* "Design and Test of the Clearing Electrodes for e-Cloud Mitigation in the e+ DAΦNE Ring", IPAC10, pp. 15151517, 2010.

[39] M. Zobov *et al*., "Operating Experience with Electron Cloud Clearing Electrodes at DAΦNE", ECLOUD12, 2012.

[40] D. Alesini *et al*., "DAΦNE operation with electron cloud clearing electrodes", *Phys. Rev. Lett*., Vol. 110, p. 124801, Mar. 2013.

[41] A. Drago, http://indico.cern.ch/event/306551/